J Toxicol Pathol 2019; 32: 105–109

Case Report

Pathological examination of spontaneous vacuolation of pancreatic acinar cells in mice

Kyohei Yasuno[1]*, Saori Igura[2], Yuko Yamaguchi[2], Masako Imaoka[1], Kiyonori Kai[1], and Kazuhiko Mori[1]

[1] Medicinal Safety Research Laboratories, Daiichi Sankyo Co., Ltd., 1-16-13 Kita-Kasai, Edogawa-ku, Tokyo 134-8630, Japan
[2] Pathology Department, BoZo Research Center Inc, Gotemba-shi, Shizuoka 412-0039, Japan

Abstract: Pancreatic acinar cell vacuolation is spontaneously observed in mice; however, the lesion is rare and has not been well documented. Herein, we present a detailed pathological examination of this lesion. Vacuoles in pancreatic acinar cells were present in 2/15 X gene knockout mice with a C57BL/6J mouse background, 4/298 ICR(CD-1) mice, 1/110 B6C3F1 mice, and 3/399 CByB6F1-Tg(HRAS)2Jic mice. The vacuoles were usually observed in a unit of the acinus, and the lesions were spread throughout the pancreas. These vacuoles contained weakly basophilic material that was positive for the periodic acid-Schiff reaction. Immunohistochemically, the vacuoles were positive for calreticulin antibody. Electron microscopy revealed globular dilatation of the rough endoplasmic reticulum (rER). According to these findings, vacuolation of pancreatic acinar cells is caused by the accumulation of misfolded proteins and enlargement of the rER. (DOI: 10.1293/tox.2018-0065; J Toxicol Pathol 2019; 32: 105–109)

Key words: vacuolation, acinar cells, pancreas, endoplasmic reticulum, mouse

Vacuolation of pancreatic acinar cells was observed in X gene knockout (KO) mice with a C57BL/6J mouse background. Although similar lesions are empirically known to be observed in other mouse strains, these cases are rare and have not been well documented. Herein, we present a detailed pathological examination of this lesion using four strains including KO mice. We performed immunohistochemical staining and electron microscopy to examine in detail the morphological characteristics of the vacuoles in the pancreas.

Four strains of non-treated or 0.5% methylcellulose solution-treated mice were used in this study: 17-week-old male X gene KO mice with a C57BL/6J mouse background (n=15; five wild-type, five hetero-KO, and five homo-KO mice, CLEA Japan, Inc., Tokyo, Japan), 110-week-old Crlj:CD1(ICR) mice (n=298; 150 male and 148 female mice, Charles River Laboratories Japan, Kanagawa, Japan), 110-week-old B6C3F1/Crl mice (n=110, 55 male and 55 female mice, Charles River Laboratories Japan), and 34-week-old CByB6F1-Tg(HRAS)2Jic (*ras*H2) mice (n=399; 200 male and 199 female mice, CLEA Japan, Inc.). This study was approved by the Ethics Review Committee for Animal Experimentation of Daiichi Sankyo Co., Ltd. (Tokyo, Japan) and was performed in accordance with the guidelines of the Animal Care and Use Committee of Daiichi Sankyo Co., Ltd. and in compliance with the laws or guidelines relating to animal welfare including the Standards Relating to the Care and Management, etc. of Experimental Animals (Notification No. 6 of the Prime Minister's Office, Japan, March 27, 1980) and Guidelines for Animal Experimentation (Japanese Association for Laboratory Animal Science, May 22, 1987). Animals were housed in individual or pair breeding cages in an animal study room with a controlled temperature of 20 to 26°C, humidity of 30% to 70%, and a 12-h light (150 to 300 lux) and 12-h dark cycle. A certified pellet or powder diet (CRF-1, Oriental Yeast Co., Ltd., Tokyo, Japan) and tap water were provided *ad libitum*.

The mice were euthanized by exsanguination under anesthesia. The pancreases of the mice were fixed in 10% neutral-buffered formalin, embedded in paraffin, sectioned, and stained with hematoxylin and eosin (HE). Periodic acid–Schiff (PAS), alcian blue, immunohistochemistry (trypsin, carboxypeptidase A, DNA damage-inducible transcript 3 [DDIT3], and activating transcription factor 4 [ATF4]), immunofluorescence (calreticulin), and electron microscopy assays were performed in mice with acinar cell vacuolation. Alcian blue staining, immunohistochemistry, and immunofluorescence were performed using samples from the KO mice. For immunohistochemistry or immunofluorescence, following incubation of the sections with 4% Block Ace™

Received: 14 December 2018, Accepted: 15 January 2019
Published online in J-STAGE: 7 February 2019
*Corresponding author: K Yasuno
(e-mail: yasuno.kyohei.ss@daiichisankyo.co.jp)

Table 1. Protocol of Immunohistochemistry and Immunofluorescence

	Primary antibody			Secondary antibody		Antigen retrieval
	Clone	Dilution	Source		Source	
Trypsin	D-1	1:50	Santa Cruz Biotecnology Inc., Dallas, TX, USA	Histofine Simple Stain Rat MAX-PO (M)	Nichirei Biosciences Inc., Tokyo, Japan	AC, 121°C, 20 min
Carboxypeptidase A	EPR12086	1:250	Abcam plc, Cambridge, UK	Histofine Simple Stain Rat MAX-PO (R)	Nichirei Biosciences Inc., Tokyo, Japan	MW, 98°C, 20 min
Calreticulin	EPR3924	1:500	Abcam plc, Cambridge, UK	Alexa Fluor® 488 AffiniPure Goat Anti-Rabbit IgG (H+L)	Jackson ImmunoResearch Inc., West Grove, PA, USA	No treatment
DDIT3	9C8	1:200	Abcam plc, Cambridge, UK	Polyclonal Goat Anti-Rabbit Immunoglobulins/Biotinylated	Dako, Agilent Technologies, Inc., Santa Clara, CA, USA	Boiling, 95°C, 15 min
ATF4	Polyclonal	1:100	Abcam plc, Cambridge, UK	Polyclonal Goat Anti-Rabbit Immunoglobulins/Biotinylated	Dako, Agilent Technologies, Inc., Santa Clara, CA, USA	Boiling, 95°C, 15 min

DDIT3, DNA damage-inducible transcript 3; ATF4, activating transcription factor 4; AC, autoclave, citrate buffer (pH 6.0); MW, microwave, citrate buffer (pH 6.0); boiling, Target Retrieval Solution (Dako Agilent Technologies, Inc., pH 6.1 [ATF4] or 9 [DDIT3])

Table 2. Incidence of Vacuolation of Pancreatic Acinar Cells in Mice

Strain	Number of animals with vacuolation			
	Male	Female	Total	Ratio
Knockout mice with a C57BL/6J mouse background	2 (15)*	NE	2 (15)	13.3%
CD1(ICR) mice	0 (150)	4 (148)	4 (298)	1.3%
B6C3F1/Crl mice	0 (55)	1 (55)	1 (110)	0.9%
*ras*H2 mice	2 (200)	1 (199)	3 (399)	0.8%

*Two hetero-knockout (KO) mice were positive from five wild-type, five hetero-KO, and homo-KO mice; NE: not examined. The numbers in parentheses denote the numbers of animals examined.

(Snow Brand Milk Products Co., Ltd., Sapporo, Japan) and Protein Block Serum (Dako, Agilent Technologies, Inc., Santa Clara, CA, USA) or Goat Serum (Dako, Agilent Technologies, Inc.), dewaxed sections were incubated with the antibodies summarized in Table 1. The immunoenzyme polymer method, indirect immunofluorescence method, Mouse on Mouse polymer IHC Kit (Abcam plc., Cambridge, UK), and labeled streptavidin-biotin (LSAB) staining method were used for anti-trypsin and anti-carboxypeptidase A antibodies, anti-calreticulin antibody, anti-DDIT3 antibody, and anti-ATF4 antibody, respectively. After immunoreaction with the secondary antibodies summarized in Table 1, the sections were stained with diaminobenzidine and counterstained with Mayer's hematoxylin, except for the calreticulin assay. For the calreticulin assay, fluorescence was analyzed using a BZ-X700 microscope (Keyence Corporation, Osaka, Japan).

Portions of the 10% neutral-buffered formalin-fixed tissue specimens from several pancreas samples with acinar vacuolation of KO and *ras*H2 mouse were cut into cubes of 1 mm^3, refixed in 2.5% glutaraldehyde, and postfixed in 1% OsO_4 for 2 h. These specimens were then dehydrated through ascending grades of alcohol and embedded in epoxy resin. Ultrathin sections were double-stained with uranyl acetate and lead citrate and examined using an H-7500 transmission electron microscope (Hitachi High-Technologies Corporation, Tokyo, Japan) at 80 kV.

Light microscopy showed vacuoles in pancreatic acinar cells in all examined strains. The incidence in each strain is summarized in Table 2. No vacuolation was observed in any other organs of these animals. The vacuoles were usually observed in a unit of the acinus, and the lesions were spread through the pancreas geographically (Fig. 1). The vacuoles were located between the basal ergastoplasm and luminal zymogen granules in the acinar cells and were uniformly sized (Fig. 2). Decreased zymogen granules were observed in these cells, but single-cell necrosis was not observed. The vacuoles contained weakly basophilic material which was positive for the PAS reaction (Fig. 3) and negative for Alcian blue staining. In immunohistochemistry and immunofluorescence assays of the KO mice, the vacuoles were positive for calreticulin antibody (Fig. 4) and negative for trypsin, carboxypeptidase A, DDIT3, and ATF4 antibodies. Electron microscopy revealed globular dilatation of the rough endoplasmic reticulum (rER) up to a diameter of 1 to 2 µm, and the rER occasionally showed a beaded appearance (Fig. 5). Coincident with the light microscopy findings, these cells lacked most of their zymogen granules. Accumulation of proteinaceous material showing mosaic electron density was observed in the enlarged rER (Fig. 6). Other microorganisms did not show any abnormalities.

Pancreatic acinar cell vacuolation occurs through a degenerative process that leads to the intercellular accumulation of different types of substances, including fluids, lipids, phospholipids, and glycoproteins[1]. It is impossible to conclusively characterize the nature of the intracytoplasmic

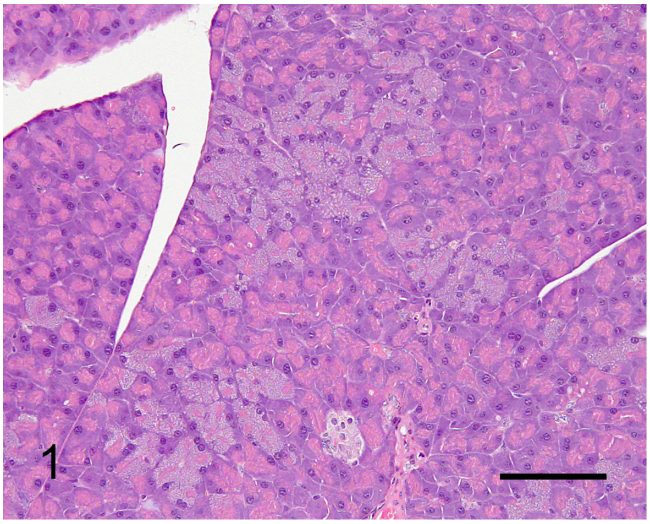

Fig. 1. Light micrograph of the pancreas of a knockout (KO) mouse with a C57BL/6J mouse background showing vacuolation of the acinar cells. Vacuolar lesions were observed throughout the pancreatic lobules. Hematoxylin and eosin (HE) staining. Scale bar=100 µm.

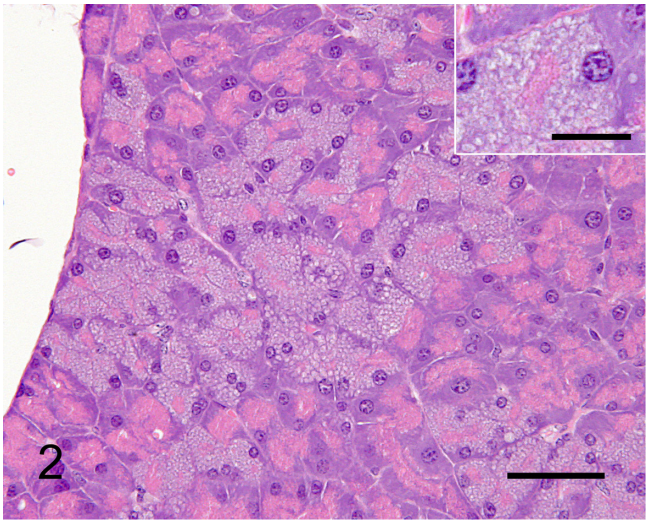

Fig. 2. Higher magnification of Fig. 1. Microvacuoles contained weakly basophilic material and were mainly observed between the basal ergastoplasm and the apical lumen in the acinar cells. The vacuoles showed a uniform size. Note the decrease of zymogen granules in these cells. HE. Bar=50 µm (inset, scale bar=20 µm).

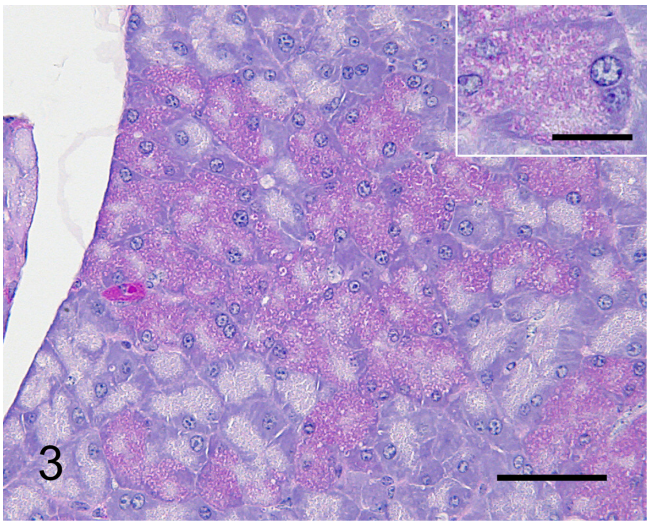

Fig. 3. Microvacuoles were weakly positive for periodic acid–Schiff reaction in KO mice. Scale bar=50 µm (inset, scale bar=20 µm).

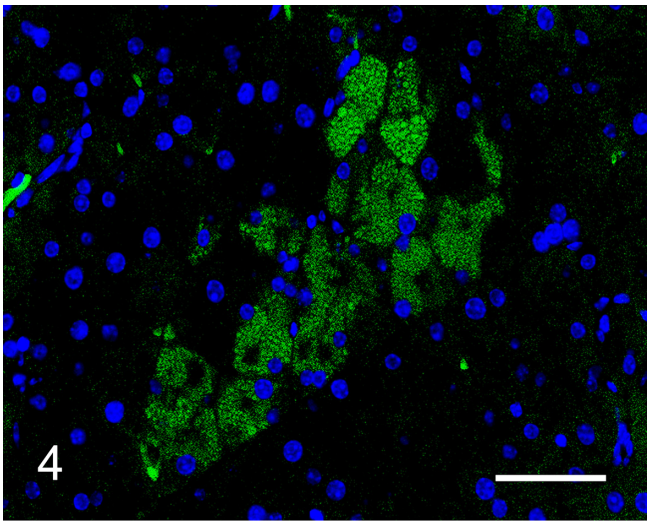

Fig. 4. Microvacuoles contained calreticulin, a molecular chaperon protein in endoplasmic reticulum in KO mice. Immunofluorescence. Scale bar=50 µm.

vacuoles by HE staining. Using electron microscopy, these vacuoles could be distinguished based on the enlargement of the ER[2, 3], Golgi apparatus[4], mitochondria[5], and autophagic vacuole or the accumulation of lipids[6, 7]. In the present study, the surface of the vacuoles was studded with ribosomes and was positive for calreticulin, a molecular chaperone protein located inside the rER[8, 9], indicating that the vacuoles originated from the rER. A positive PAS reaction and ultrastructural mosaic electron density indicated the accumulation of proteinaceous material in the vacuoles. The zymogen granules in the acinar cells show varied electron density and become dense during their maturation, as observed by electron microscopy[10]. Therefore, the vacuoles in the present study might contain digestive enzymes at a variety of development stages. However, the vacuoles were negative for mature digestive enzymes such as trypsin and carboxypeptidase A[11] according to immunohistochemistry. Since decreased zymogen granules were observed in the vacuolated cells, it was speculated that digestive enzyme formation was dysfunctional.

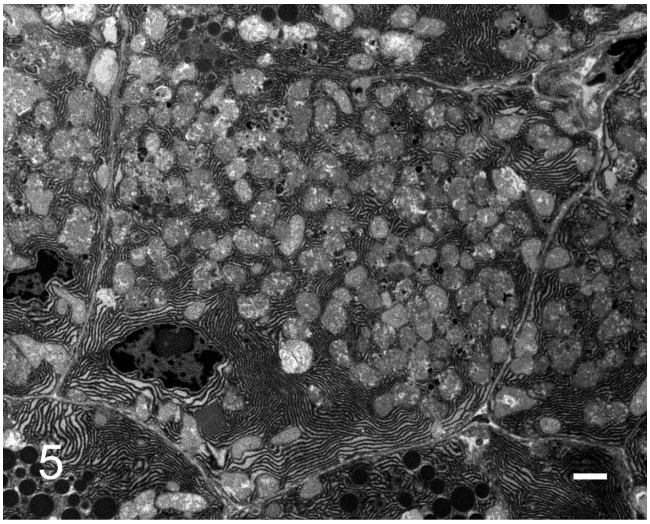

Fig. 5. Electron micrograph of an acinar cell with microvacuoles in the cytoplasm of a KO mouse. Many microvacuoles were observed between the basal ergastoplasm and the apical lumen. Scale bar=2 μm.

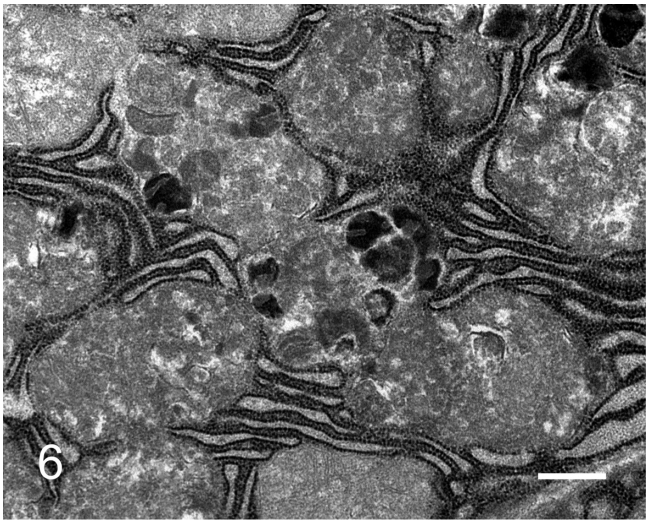

Fig. 6. Higher magnification of Fig. 5. The rough endoplasmic reticulum was dilated and contained a proteinaceous substance showing mosaic electron density. Note studded ribosomes at the surface of the vacuoles. Scale bar=50 nm.

In acinar cells, secretory protein transcripts pass across the ER, where folding, glycosylation, and disulfide bond formation occur[12]. Thus, the ER forms the first compartment of the secretory pathway, followed by the formation of the Golgi apparatus, the condensing of vacuoles, and the secretion of granules. Protein folding in the ER is affected by many parameters, including pH, calcium levels, oxidative stress, and the availability of chaperones, foldases, and protein disulfide isomerases. An imbalance of these parameters leads to an accumulation of misfolded proteins and induces ER stress[13]. A major component of the ER stress response is the unfolded protein response (UPR), which maintains an equilibrium between the capacity and demand for protein folding within the ER[14]. At low-to-moderate levels of ER stress, the UPR increases the folding capacity of the ER by the enlargement of the ER and the increased synthesis of molecular chaperones and foldases[15, 16]. Calreticulin is a chaperone found in sensor proteins that recognizes misfolded proteins and prevents them from being exported from the ER to the Golgi apparatus[8, 9]. In the present study, calreticulin was observed in the enlarged rER, indicating an accumulation of misfolded proteins and ER stress in vacuolated cells. However, DDIT3 and ATF4, known markers of ER stress in biological studies[17], were negative according to the immunohistochemistry assay. DDIT3 and ATF4 are proteins involved in the protein kinase R-like endoplasmic reticulum kinase (PERK) pathway which induces apoptosis through regulation of the Bcl-2 family and reactive oxygen species (ROS) formation[18]. The lack of expression of these pro-apoptotic markers led to a lack of necrosis in the present case; however, further examination of other ER stress proteins, such as inositol-requiring enzyme 1 and ATF6, is required in order to understand the pathogenesis of vacuoles.

The typical characteristics of vacuolation were observed in all tested strains, implying that this lesion is a rare spontaneous lesion in mice. In our study, this lesion was not found to be dependent on sex or age. KO mice showed a higher incidence of vacuolation than other strains; however, this is likely to be due to the number of KO mice examined in this study. More data on C57BL/6J mice is required to discuss strain dependency. In KO mice, the X gene is not expressed in the pancreas but is mainly expressed in the aorta and ovaries (data not shown), suggesting that this lesion is not related to the knockout of the X gene. It is well known that chronic ER stress causes acinar cell apoptosis, which can lead to necrosis, a severe inflammatory response, acute respiratory distress, or life-threatening multiorgan failure[13]. Pancreatitis is uncommon in mice, only occurring in 3% to 5% of the control group in 2-year carcinogenicity studies[19]; however, its relationship with vacuolation is not known. In the present study, although vacuolation was observed in 110-week-old mice, these mice did not show any signs of necrosis or inflammation, suggesting that this lesion does not develop into an irreversible injury. In addition, lesions were observed in a unit of the acinus, and no mice showed diffuse vacuolation as an end stage of this lesion. Although the progress of this lesion has yet to be fully elucidated, our data suggest that vacuolation is not a progressive, severe, or degenerative lesion.

In conclusion, the vacuoles in the present study were found to be positive for the PAS reaction and consisted of an enlarged rER, which was caused by an accumulation of misfolded proteins.

Disclosure of Potential Conflicts of Interest: The authors declare that there are no conflicts of interest.

Acknowledgments: The authors would like to thank Ms. Shinobu Hakamata, Ms. Rumiko Ishida, Mr. Shigehito Takeshita (Daiichi Sankyo Co., Ltd.), and Ms. Keiko Okado (Daiichi Sankyo RD Novare Co., Ltd.) for their excellent support in the pathological examination and their assistance in the collection of specimens; Dr. Takuya Doi (LSI Medience Corporation) for his kind advice; and Prof. Kinji Shirota (Azabu University) for providing anti-trypsin and anti-carboxypeptidase A antibodies.

References

1. Nolte T, Brander-Weber P, Dangler C, Deschl U, Elwell MR, Greaves P, Hailey R, Leach MW, Pandiri AR, Rogers A, Shackelford CC, Spencer A, Tanaka T, and Ward JM. Nonproliferative and proliferative lesions of the gastrointestinal tract, pancreas and salivary glands of the rat and mouse. J Toxicol Pathol. **29**(Suppl): 1S–125S. 2016. [Medline] [CrossRef]
2. Wallig MA, Gould DH, and Fettman MJ. Selective pancreato-toxicity in the rat induced by the naturally occurring plant nitrile 1-cyano-2-hydroxy-3-butene. Food Chem Toxicol. **26**: 137–147. 1988. [Medline] [CrossRef]
3. Lugea A, Tischler D, Nguyen J, Gong J, Gukovsky I, French SW, Gorelick FS, and Pandol SJ. Adaptive unfolded protein response attenuates alcohol-induced pancreatic damage. Gastroenterology. **140**: 987–997. 2011. [Medline] [CrossRef]
4. Schmidt K, Schrader M, Kern HF, and Kleene R. Regulated apical secretion of zymogens in rat pancreas. Involvement of the glycosylphosphatidylinositol-anchored glycoprotein GP-2, the lectin ZG16p, and cholesterol-glycosphingolipid-enriched microdomains. J Biol Chem. **276**: 14315–14323. 2001. [Medline] [CrossRef]
5. Sano T, Ozaki K, Matsuura T, and Narama I. Giant mitochondria in pancreatic acinar cells of alloxan-induced diabetic rats. Toxicol Pathol. **38**: 658–665. 2010. [Medline] [CrossRef]
6. Haschek WM, Rousseaux CG, and Wallig MA. Pancreas. In: Fundamentals of Toxicologic Pathology, 2nd ed. WM Haschek, CG Rousseaux, and MA Wallig (eds). Academic Press, Burlington. 237–259. 2010.
7. Longnecker DS, Crawford BG, and Nadler DJ. Recovery of pancreas from mild puromycin-induced injury. A histologic and ultrastructure study in rats. Arch Pathol. **99**: 5–10. 1975. [Medline]
8. Trombetta ES. The contribution of N-glycans and their processing in the endoplasmic reticulum to glycoprotein biosynthesis. Glycobiology. **13**: 77R–91R. 2003. [Medline] [CrossRef]
9. Michalak M, Corbett EF, Mesaeli N, Nakamura K, and Opas M. Calreticulin: one protein, one gene, many functions. Biochem J. **344**: 281–292. 1999. [Medline] [CrossRef]
10. Alder G, and Kern HF. The human exocrine pancreas in health and disease. In: Ultrastructure of the Extraparietal Glands of the Digestive Tract. A Riva, and PA Motta (eds). Kluwer Academic Publishers, Boston. 115–146. 1990.
11. Christianson DW, and Lipscomb WN. Carboxypeptidase A. Acc Chem Res. **22**: 62–69. 1989. [CrossRef]
12. Jamieson JD, and Palade GE. Synthesis, intracellular transport, and discharge of secretory proteins in stimulated pancreatic exocrine cells. J Cell Biol. **50**: 135–158. 1971. [Medline] [CrossRef]
13. Logsdon CD, and Ji B. The role of protein synthesis and digestive enzymes in acinar cell injury. Nat Rev Gastroenterol Hepatol. **10**: 362–370. 2013. [Medline] [CrossRef]
14. Cao SS, and Kaufman RJ. Unfolded protein response. Curr Biol. **22**: R622–R626. 2012. [Medline] [CrossRef]
15. Dorner AJ, Wasley LC, and Kaufman RJ. Increased synthesis of secreted proteins induces expression of glucose-regulated proteins in butyrate-treated Chinese hamster ovary cells. J Biol Chem. **264**: 20602–20607. 1989. [Medline]
16. Kozutsumi Y, Segal M, Normington K, Gething MJ, and Sambrook J. The presence of malfolded proteins in the endoplasmic reticulum signals the induction of glucose-regulated proteins. Nature. **332**: 462–464. 1988. [Medline] [CrossRef]
17. Oslowski CM, and Urano F. Measuring ER stress and the unfolded protein response using mammalian tissue culture system. Methods Enzymol. **490**: 71–92. 2011. [Medline] [CrossRef]
18. Tabas I, and Ron D. Integrating the mechanisms of apoptosis induced by endoplasmic reticulum stress. Nat Cell Biol. **13**: 184–190. 2011. [Medline] [CrossRef]
19. Maronport RR. Exocrine and endocrine pancreas. In: Pathology of the Mouse. RR Maronport (ed). Cache River Press, Vienna. 185–205. 1999.